

Versuch A1– Spektroskopie der Sonne

Betreuung & Kontakt:

Miguel A. Urbaneja

miguel.urbaneja-perez@uibk.ac.at

Version FEB.2024

Contents

| | | |
|----------|--------------------------------------------------|-----------|
| 1 | Introduction | 3 |
| 2 | Historical overview | 3 |
| 3 | Principles of spectrographs | 4 |
| 3.1 | The grating as a dispersive element | 5 |
| 3.1.1 | The Echelle spectrograph | 6 |
| 4 | Physical background of solar spectroscopy | 6 |
| 4.1 | Spectral lines - The curve of growth | 7 |
| 5 | The experiment | 8 |
| 5.1 | Summary | 8 |
| 5.2 | Data collection | 8 |
| 5.3 | Data processing | 11 |
| 5.4 | Data analysis | 11 |
| 6 | Evaluation of the experiment | 12 |

1 Introduction

Spectroscopy is a fundamental technique used in astrophysics to analyze the electromagnetic radiation emitted by astronomical objects. The Sun, a G-type main-sequence star (G2V), serves as the primary source of energy for the Earth and the solar system. Understanding its composition, temperature, and dynamics is crucial for elucidating various astrophysical phenomena and their impacts on Earth's environment and technology.

The study of solar spectroscopy involves the analysis of the Sun's spectrum, which provides valuable information about its chemical composition, temperature distribution, magnetic fields, and physical processes occurring within its layers. The solar spectrum consists of electromagnetic radiation spanning a wide range of wavelengths, from radio waves to gamma rays, each revealing different aspects of solar phenomena. The Sun's spectrum exhibits absorption lines, emission lines, and continuum radiation across various spectral regions. These features arise from interactions between photons and atoms, ions, and molecules in the Sun's atmosphere. The absorption lines correspond to wavelengths at which certain elements in the solar atmosphere absorb specific frequencies of light, whilst emission lines indicate the release of energy as photons during atomic transitions.

Solar spectroscopy relies on spectroscopic techniques, involving spectrographs, which disperse incoming light into its constituent wavelengths, enabling detailed analysis and interpretation of solar spectra. By examining the intensity, shape, and position of spectral lines, it is possible to infer properties such as chemical abundances, temperature gradients, and magnetic field strengths within the Sun's atmosphere.

In this experiment, we aim to explore the principles of solar spectroscopy by acquiring and analyzing solar spectra using an Echelle spectrograph. By observing and interpreting the solar spectrum, we seek to identify prominent spectral lines corresponding to a given ionization stage of a specific element, iron (Fe). The measurements of the properties of these Fe lines will allow the determination of the effective temperature of the Sun as well as the total number of atoms of Fe, relative to the number of H atoms, in the atmosphere of the Sun. Through hands-on experimentation and data analysis, this study provides students with practical insights into the techniques and principles of astronomical spectroscopy while fostering a deeper understanding of solar physics and astrophysical techniques.

2 Historical overview

The roots of solar spectroscopy trace back to the early 17th century when astronomers began to explore the nature of sunlight using prisms and simple spectrometers. In 1666, Sir Isaac Newton demonstrated that white light could be separated into its constituent colours, laying the foundation for the field of spectroscopy. However, it wasn't until the 19th century that significant progress was made in unravelling the mysteries of the solar spectrum.

William Hyde Wollaston (1766, East Dereham/Norfolk – 1828, London) discovered several dark lines in the spectrum of the Sun in 1802, thus identifying for the first time absorption lines. Independently, Joseph von Fraunhofer (1787, Straubing – 1826, Munich) made a similar discovery in 1813. Fraunhofer's utilization of these lines for optical glass measurements and subsequent publication of the results led to the absorption lines in the solar spectrum being named after him (i.e. the Fraunhofer lines).

Father Angelo Secchi (1818, Reggio Emilia–1878, Rome) further decomposed the light of stars using prisms. By analyzing the distribution of colour patterns and dark absorption lines, he classified stars into four distinct spectral classes. It is sometimes wrongly noted that he purportedly examined the chemical composition of the Sun. At that time, it was not feasible for him to do so, even though he was aware of Kirchhoff and Bunsen's 1859 discovery that different chemical elements impart characteristic colours to a gas burner's flame. Knowledge regarding not only the chemical composition but also the pressure and temperature conditions in stellar atmospheres governing line formation was still lacking. Robert Wilhelm Eberhard Bunsen (1811, Göttingen–1899, Heidelberg) primarily worked with salts of solid substances, but the metals contained in these salts were of marginal importance for stellar spectroscopy. Moreover, the broad bands of M-type stars could not be assigned to any known chemical element. Today, we understand that these bands are series of rotational and vibrational modes of molecules such as CH (previously discovered as "G band" in the Sun by Fraunhofer), C₂, CO, TiO, and O₂. Secchi's contributions in the field of solar spectroscopy were groundbreaking, positioning him as a pioneer of spectroscopic analysis, and laying the groundwork for modern research in the field.

3 Principles of spectrographs

The principle of spectroscopy always involves the decomposition of light (not only the visible part) into its components with different wavelengths. This separation is achieved using various media, referred to as dispersing elements. The resolution (how much the incoming light splits) depends on the design and can also be a nonlinear function of the wavelength. In such cases, it is referred to as a nonlinear dispersion relation.

The oldest known dispersing element in use is the prism. It capitalizes on the fact that the refractive index of most glasses is lower for low-frequency (red) light than for high-frequency (blue) light. As a result, when light enters the prism at an angle, it undergoes splitting within the glass body. Integrating this system into the optical path of a standard optical imaging instrument (e.g., a telescope) yields small spectra instead of point-like images of objects (e.g., stars). The main drawbacks of this system are its highly nonlinear dispersion properties.

A simple optical spectrometer comprises only a few components:

- An entrance to the instrument, that defines the field of view and regulates the amount of light that reaches subsequent parts of the instrument.
- A collimator lens, which parallelizes the divergent incident light; achromatic lenses are necessary to ensure this condition over a wide range of wavelengths.
- A light-dispersing element (a prism, for example) to disperse the radiation to be analyzed.
- A camera lens, to focus the beam into the detector.
- An eyepiece to view and measure the spectrum directly with the eye. Alternatively, it can be projected onto a screen or detector using additional lenses.

3.1 The grating as a dispersive element

When coherent, monochromatic light passes through two narrow, parallel slits, an interference pattern of bright and dark fringes emerges on an observation screen behind the plane of the slits due to the interference of light passing through the two openings. Light incident on a diffraction grating, a type of dispersive element widely used in Astronomy, is diffracted akin to the double-slit experiment, where the resulting elementary waves interfere to form a spectrum. In contrast to the spectra from the double slit experiment, the main maxima result sharper with increasing grating slits, while the secondary maxima become more numerous but weaker. Consequently, the resolving power increases. Crucial aspects for the quality and resolution of a spectrum are:

- The number of lines on the grating.
- The coherence of the incoming light – maintaining a perfect parallel beam onto the grating is essential.

The basic equation governing the behaviour of a grating can be written as

$$m\lambda = f(\alpha, \beta)$$

where m , an integer number, is called the order, λ is the wavelength of the radiation, α is the angle of incidence of the incoming light into the grating, and β is the outgoing angle. It can be seen from this equation that, for a given order, there is a unique position in the focal plane for each wavelength (since the incident angle is the same for all wavelengths).

Blaze gratings are reflection gratings optimized to provide the maximum light efficiency for a specific combination of wavelength and order. Like all optical gratings, they have a constant line spacing (grooving). The grooves have a cross- section resembling a non-equilateral triangle. The so-called blaze angle is one formed by the normal to the hypotenuse and the normal to the longest side of the triangle.

By constructing the grating for a specific blaze angle, the intensity of the diffracted radiation reaches a maximum value in the desired diffraction order; the grating achieves high efficiency in the desired wavelength range, whilst at the same time, extremely low efficiency can be expected at other wavelength ranges.

3.1.1 The Echelle spectrograph

To achieve very high resolutions in astronomical observations, spectrographs operating at high orders are widely used. However, this high resolution comes at the cost of significantly reduced intensity. A second important drawback is the overlapping of orders: the red light of one order can potentially fall onto the blue light of the following order at the same location on the detector. This issue is mitigated by utilizing the full 2D extension for the detector.

In an Echelle spectrograph, a second grating, generally with lower resolution, is placed behind the first one, with its dispersion direction perpendicular to that of the first grating. As a result, the light beam undergoes a second dispersion, this time in a perpendicular axis to the previous one. The resulting spectra of the individual orders are arranged on top of each other in the focal plane. However, the combination of two gratings exhibits nonlinear dispersion terms, resulting in curved spectra.

4 Physical background of solar spectroscopy

The physics of the formation of the solar spectrum is governed by the principles of thermal radiation, similar to that of Planck's radiation. The effective temperature (i.e. the temperature of a black body that would radiate the same total amount of energy per unit of time) of the solar atmosphere is approximately 5778 K. When there is gas above such a layer, this gas absorbs radiation at wavelengths determined by the energy states of electron transitions within the atom. If the gas has the same temperature as the underlying layer and is in thermodynamic equilibrium (i.e., collision rates are sufficiently high and external effects are negligible), it emits the same number of photons at that wavelength. An observer would not detect any absorption lines because absorptions and emissions would balance each other out.

However, in the presence of a temperature gradient, the occupancy of higher states is lower (recall Boltzman's equation). Consequently, we observe absorption lines since fewer photons are emitted than those absorbed coming from the inside. Since the photosphere of the Sun becomes cooler outwardly, we observe these absorption lines.

When measuring a line, one determines the so-called equivalent width (EW). One assumes a background source of constant intensity, which is attenuated by foreground material around a certain wavelength λ_0 (the position of the line *line core*). The total area between the background source with intensity $I_0 = \text{constant}$ and the actual intensity profile $I(\lambda)$ is given as:

$$\text{EW} = \int \frac{I_0 - I_\lambda}{I_0} d\lambda$$

The equivalent width EW geometrically corresponds to the length of a rectangle of height unity with the same area as the absorbed intensity. Physically, the equivalent width represents a measure of the energy absorbed in the line. The EW of a line provides a measure of the total number of absorbing atoms in the lower excitation states of the atom transitioning to a higher state. In a plasma in thermodynamic equilibrium, the occupancy of the upper level is usually lower than that of the lower level. There are no saturations or degeneracies, so the density of the upper level is not significant.

In a gas layer of thickness ds , the absorption depends on the (wavelength-dependent) absorption coefficient κ_λ . This coefficient is a function of the number of atoms N_i in the relevant excitation state responsible for the absorption process, as well as the oscillator strength for the transition. The EW of an absorption line naturally changes with increasing N_i (relative to a gas column with volume V). The function describing this change is called the *curve of growth*.

4.1 Spectral lines - The curve of growth

We have previously discussed a basic view of the formation of absorption lines under the assumption of local thermodynamic equilibrium. From the physical point of view, the occurrence of these lines represents a decrease in radiation flux. Doubling the layer thickness (or, equivalently, doubling the particle density while maintaining the layer thickness) increases the equivalent width by a factor of 2, provided the absorbing gas layer is optically thin. In general, for optically thin lines, there is a direct proportionality between the equivalent width and the number of atoms involved in the absorption process along the line of sight.

Since the occupation of atomic states is described by the Boltzmann statistics, the EW of a line must be proportional to

$$EW_\lambda \propto \frac{N_{r0}}{g_{r0}} g_{rs} f_{rs} \lambda^2 \exp(-\chi_i/kT)$$

where r represents the ionization degree of the atom and s denotes the quantum description of the involved line transition (quantum numbers of both levels). The oscillator strengths f and degeneracy g (or their required product), as well as the excitation energy of the level χ , are obtained from laboratory measurements and theoretical calculations (solution of the Schrödinger equation) of the systems.

However, at some point, the lines become so strong that the optically thin approximation is no longer valid. Hence, *saturation* occurs. The effect of saturation on the EW of the line depends on the types of broadening mechanisms acting on the line (Doppler broadening due to thermal motions, Stark broadening due to pressure, and so on). This behaviour of the EW of the lines for the number density of absorbers is described by the so-called curve of growth.

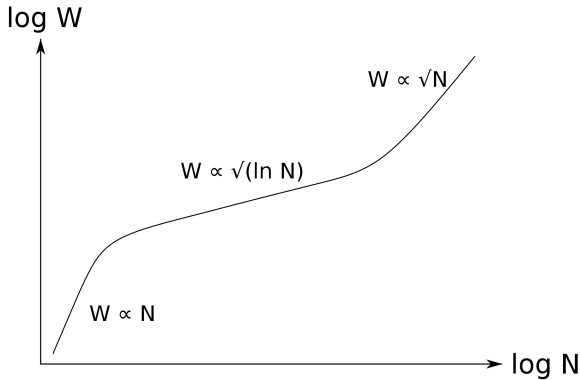


Figure 1: A generic curve of growth, illustrating the different regimes. (Source: Wikipedia).

5 The experiment

5.1 Summary

The goal of the experiment is to determine the effective temperature and the ratio of iron to hydrogen atoms (the iron abundance) in the photosphere of the Sun. Before performing the actual measurements, a set of science and calibration frames will be taken with the instrument/telescope, and subsequently processed with specific software routines created for that end.

Once a wavelength-calibrated, flux-normalized spectrum of the Sun is obtained, more than 200 Fe I lines should be measured, in order to determine their central wavelength and EW. With this information in hand, along with the corresponding atomic data given in a complementary file (not included in this document), the analysis should be performed through the curve of growth.

5.2 Data collection

In astrophysics, digital cameras, such as Charge-Coupled Devices (CCDs), and in more recent years Complementary Metal- Oxide-Semiconductor (CMOS) detectors, play a crucial role in collecting data from astronomical objects. These detectors are sensitive to photons in wide ranges of the electromagnetic spectrum. The process begins with exposing the detector to light from the target object. As photons hit the detector, they generate electrons, producing an electric signal that can be recorded.

Photon statistics, particularly the Poisson distribution, play a crucial role in understanding the fundamental nature of light and its detection by digital cameras. The Poisson distribution describes the probability of observing a certain number of events (photons, in this case) within a given time or space interval, given the average rate of occurrence. Each pixel in a detector collects photons from the illumination source, and the number of photons detected at each pixel follows a Poisson distribution. Understanding this statistical distribution is essential for accurately measuring the signal-to-noise ratio of astronomical images and for estimating uncertainties.

Besides the frames corresponding to the object of interest, several supporting frames (calibrations) need to be collected, to remove the effects introduced by the measuring process. For the particular case of spectroscopy, the following calibration frames are required:

1. Bias Frames: Bias frames are images taken with no exposure to light. They capture the electronic noise inherent in the CCD/CMOS system, including readout noise and electronic offsets. These noise sources can introduce unwanted signals into astronomical images. Bias frames help characterize and subtract this noise during data processing, ensuring more accurate measurements of the target objects.
2. Flatfield Frames: Flatfield frames are images taken to characterize the pixel-to-pixel variations in the detector response and the optical system's illumination. They are typically obtained by uniformly illuminating the spectrograph's entrance slit with a stable light source, such as a flat-field lamp or a twilight sky. Flatfield frames contain information about the instrumental and optical response across the entire detector by revealing imperfections in the CCD's response, such as dust on the optics or variations in pixel sensitivity. By dividing the raw astronomical images by flatfield frames, astronomers correct for these imperfections, ensuring that the final images accurately represent the true brightness of the astronomical objects.

As explained in previous sections, in an Echelle spectrograph, the dispersing element spreads the incoming light into multiple spectral orders. However, due to the nature of the optical setup, each spectral order appears curved on the detector. This curvature arises from the non-linear relationship between wavelength and position on the detector. When analyzing flatfield frames, one can observe the curvature present in each spectral order. To correct for the curvature several mathematical functions (e.g., polynomials) can be fit to the curvature profiles observed in the flatfield frames. By fitting these functions to the curvature of each spectral order, astronomers can establish a mathematical model that describes how the spectral features should be distributed across the detector. Once the curvature model is established these corrections can be applied to the rest of the frames. By applying the inverse transformation derived from the curvature model, we can straighten the curved spectral orders, effectively "unwarping" them and producing spectra with linear wavelength dispersion along the detector.

3. Wavelength Calibration Lamps: Wavelength calibration lamps emit light with known spectral lines at specific wavelengths. These lamps are used to calibrate the wavelength scale of spectroscopic observations. By observing the spectral lines from the lamp, astronomers can precisely determine the relationship between pixel position on the CCD and the corresponding wavelength of light. This calibration is essential for accurately measuring the spectra of astronomical objects and identifying specific features such as emission or absorption lines.

In summary, the process of data collection with astronomical cameras involves capturing images not only of celestial objects but also of several auxiliary sources, correcting for electronic noise and pixel sensitivity variations, and calibrating the wavelength scale for spectroscopic observations. Understanding photon statistics, particularly the Poisson distribution is essential for interpreting

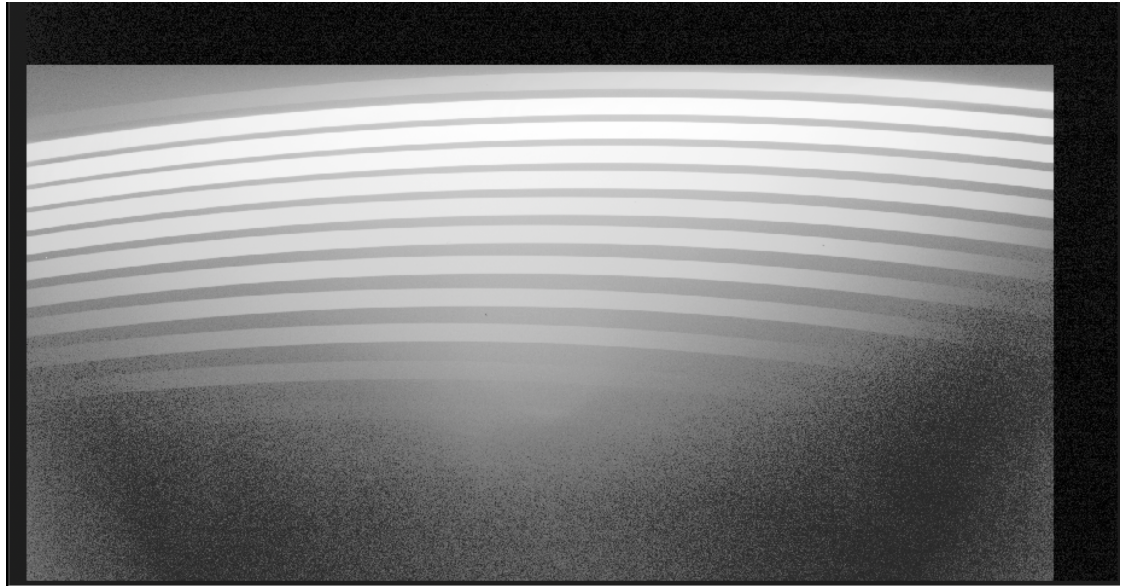


Figure 2: Flatfield image. Note that the full frame is shown in the image; this particular detector includes a region that is not illuminated. (©Miguel A. Urbaneja)

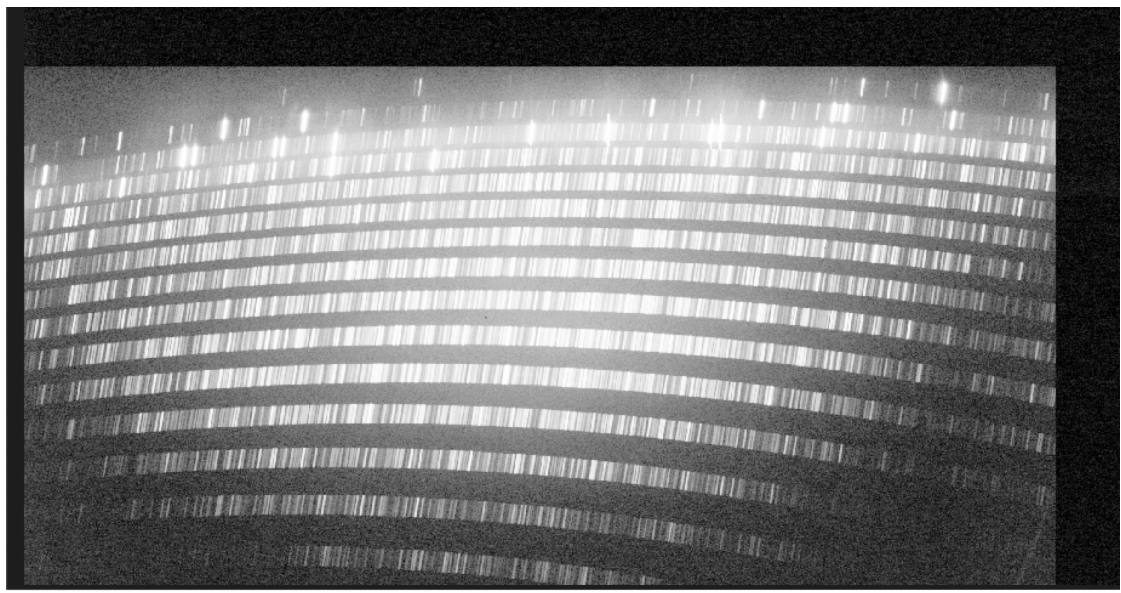


Figure 3: Wavelength calibration image (ThAr lamp). (©Miguel A. Urbaneja)

CCD data and extracting meaningful scientific information from astronomical observations.

5.3 Data processing

Processing raw images collected for stellar spectroscopy involves several key steps to produce a high-quality stellar spectrum suitable for analysis. These are the fundamental steps to be taken:

1. Bias Subtraction
2. Flatfield Correction
3. Wavelength Calibration
4. Extraction of Stellar Spectrum: once the images are bias- subtracted, flatfield-corrected, and wavelength-calibrated, the next step is to extract the stellar spectrum from the data. This involves defining regions of interest around the stellar signal on the detector and summing the flux within these regions to produce a one-dimensional spectrum.
5. Background Subtraction: background subtraction may be necessary to remove contamination from sky background or nearby stars. This step involves measuring and subtracting the background signal from the stellar spectrum to isolate the true stellar signal.
6. Normalization: normalization involves dividing the stellar spectrum by a suitable continuum reference to remove any variations in the overall flux level. This step ensures that the relative intensities of spectral features are accurately represented and facilitates the determination of the EWs of the lines.

Several IDL routines were developed specifically to be used in this practicum and are readily available for use. IDL syntax is very similar to Python. All the required steps for obtaining a fully processed solar spectrum can be performed by these routines.

5.4 Data analysis

Once the set of Fe I lines have been measured, obtaining their central wavelengths and EWs, the previously introduced curve of growth can be applied. For each line, operating the expressions introduced in the theory section, we have

$$\log \left(\frac{EW_\lambda}{\lambda} \right) = \log (\lambda g f) - \frac{5040}{T} \chi + \log (N_i/N_H)$$

this can be rearranged into

$$\log (EW_\lambda/\lambda) - \log (\lambda g f) = -\frac{5040}{T} \chi + \log (N_i/N_H)$$

This expression resembles a linear equation. The constant 5040 arises from:

$$\left[\frac{\text{eV}}{K} \right] = \left[\frac{K}{\text{eV}} \right] \times 5040 \ln(10) = \ln(\exp(1)) \times \ln(10) = 8.61734 \times 10^{-5} \left[\frac{\text{eV}}{K} \right]$$

It is very important to understand that this approximation holds only for optically thin lines, where each photon reacts with an atom only once. In the particular case of the solar spectrum, a suitable criterion for selecting thin lines is to choose those lines for which $\text{EW}_\lambda < 120 \text{ m}\text{\AA}$.

The following tasks should be performed:

1. identify weak Fe I lines and only then derive the effective temperature and the relative iron abundance.
2. With the obtained results of T and $N_{\text{Fe}}/N_{\text{H}}$ and all lines, plot the classic growth curve $y = \log(W_\lambda/\lambda)$ vs. $x = [\log(\lambda g f) + \log(N_{\text{Fe}}/N_{\text{H}})T\chi - 5040/T]$. By comparing with the theoretical growth curve, identify those lines that you might have included but still present saturation.
3. Eliminate these lines and repeat the initial analysis step without them. Consequently, you should refine the result for T and $N_{\text{Fe}}/N_{\text{H}}$. Create the graph (always with a 1:1 ratio on the axes) of the growth curve after this correction with all lines again. Elimination of saturated lines: Optically thin lines closely follow the linear trend (see theoretical growth curve). Once the lines saturate, a significant flattening of the curve can be observed. With a true 1:1 ratio of the axes of the growth curve, one can imagine an auxiliary line with a 45° slope to better observe the trend in the linear region.

6 Evaluation of the experiment

I will follow the general rules defined for FP1 for grading the experiment. Since this is the first contact of students with data collection and processing in Astrophysics, I give particular emphasis to a clear understanding of the particularities of data processing and analysis.